Polar order in columnar phase made of polycatenar bent-core molecules

Ewa Gorecka,[1,*] Damian Pociecha,[1] Joanna Matraszek,[1] Jozef Mieczkowski,[1] Yoshio Shimbo,[2] Yoichi Takanishi,[2] and Hideo Takezoe[2]

[1]*Chemistry Department, Warsaw University, Aleja Zwirki i Wigury 101, 02-089 Warsaw, Poland*

[2]*Department of Organic and Polymeric Materials, Tokyo Institute of Technology, O-okayama, Meguro-ku, Tokyo 152-8552, Japan*

(Received 22 December 2005; published 16 March 2006)

Columnar phases made of polycatenar molecules with bent-shaped mesogenic cores are studied. The polar order in this system is associated with the change of the column building blocks from flat disks (Col_h phase) into cones (Col_hP_A phase), which allows for axial polarization of the columns. The nature of the Col_h and Col_hP_A phase transition changes from first order for short homologues to continuous for the longest one. This can be attributed to decreasing intercolumnar interactions due to broadening of the columnar scaffold made of partially melted terminal alkyl chains. Decrease of intercolumnar interactions is also responsible for a strong increase of the pretransitional fluctuations in the Col_h phase. The mesophase observed for the longest homologues is reminiscent of the relaxor phase observed for solid crystals.

DOI: 10.1103/PhysRevE.73.031704 PACS number(s): 61.30.Cz, 64.70.Md, 77.84.Nh, 77.22.Gm

INTRODUCTION

The polar order in soft matter has been extensively studied for liquid crystals. For a long time polar order was associated with breaking of the chiral symmetry; this approach has been widely applied to obtain ferroelectric [1] and antiferroelectric [2] lamellar and even columnar mesophases [3,4]. In 1996, for the first time, a switchable polar smectic phase was reported also in an achiral molecular system [5,6], where the ordering of dipoles resulted from restricted molecular rotation due to the steric interactions of bent-core molecules. Recently ferroelectric switching has also been reported in columnar phases made of achiral molecules; for these materials the spontaneous electric polarization along the columns originates in soft intermolecular interactions: the net of hydrogen bonds [7,8] or assembling of bent-core polycatenars (molecules having multiple terminal chains) into conelike units [9]. Here we report the complex thermodynamics of polar order development in homologous series of polycatenar compounds. In the studied materials the polar structure grows from a paraelectric phase through either a discontinuous or continuous phase transition. In the case of the discontinuous phase transition the antiferroelectric phase is obtained below the paraelectric one, while the properties of the polar phase that enters through the continuous phase transition in many aspects recall those of disordered relaxor phases [10].

RESULTS AND DISCUSSION

In all materials of the studied homologous series (Fig. 1; Table I) below the isotropic phase three columnar phases were detected: the Col_h, Col_hP_A, and Col_X phases. The Col_h phase is paraelectric while the Col_hP_A phase is axially polar and switchable under electric field. The rather high threshold field is required for switching; in the $n=16$ homologue a saturated current peak is obtained for about 20 V μm^{-1} and even higher fields are necessary for shorter homologues. For the $n=16$ material the spontaneous polarization is ~ 250 nC cm^{-2} and decreases to zero on approaching the Col_h phase. Previous x-ray studies confirmed a strictly hexagonal arrangement of columns for both Col_h and Col_hP_A phases [9]. Assuming 1 g cm^{-3} density of material it can be deduced that in all phases the column stratum is made of 3–4 molecules, which are arranged into flat disks in the Col_h phase and into cones in the Col_hP_A phase (Fig. 1). The change of column building blocks from flat disks into cones is followed by monitoring the temperature variation of the Bragg reflection with index (10), related to the intercolumn distance. This distance decreases profoundly at the Col_h-Col_hP_A phase transition (Fig. 2), as expected for disks deforming into cones. The decrease is either stepwise (for homologues $n=8,12,14$) or continuous (homologue $n=16$). The cone angle obtained by comparing the column diameters in the Col_h and Col_hP_A phases near the transition point is in the range of $130°-140°$ for all homologues. The crossover from discontinuous to continuous Col_h-Col_hP_A phase transi-

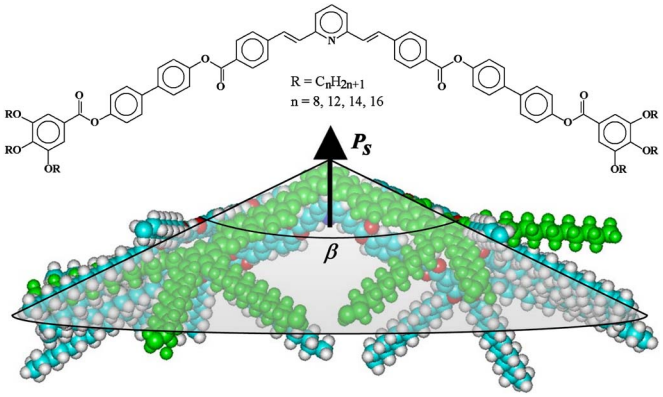

FIG. 1. (Color online) General formula of studied polycatenar compounds. Below, the arrangement of molecules into a conelike unit is shown; β denotes the cone angle. Cone units are arranged in columns with noncompensated electric polarization P_s.

*Email address: gorecka@chem.uw.edu.pl

TABLE I. Phase transition temperatures (°C) and, in parentheses, their thermal effects (J g^{-1}) for studied materials.

n	Melting point	Col_X	Col_hP_A	Col_h	Iso
8	89.6 (11.6)	128.1 (0.1)	147.3 (1.8)	189.5 (1.0)	
12	65.0 (15.5)	83.8 (6.6)	137.2 (1.5)	197.4 (1.2)	
14	34.0 (17.1)	83.7 (6.5)	122.5 (1.1)	187.3 (0.9)	
16	58.2 (20.3)	90.2 (8.2)	123.2 (1.5)	174.0 (0.9)	

tion, with elongation of terminal chains is also clearly visible in calorimetric studies (Fig. 3). For the shortest homologue, $n=8$, at the Col_h-Col_hP_A phase transition a sharp peak due to the latent heat with almost no heat capacity (c_p) anomalies is observed, as well as pronounced hysteresis of the transition temperature (T_c) for cooling and heating scans. The hysteresis diminishes and the peak develops c_p wings for longer homologues and for the $n=16$ material no hysteresis is seen and a broad c_p anomaly at both side of T_c is detected. Strong c_p anomalies are characteristic of continuous (second-order) phase transitions; the temperature hysteresis for heating and cooling scans is possible only for discontinuous (first-order) phase transitions. The polar instability associated with the Col_h-Col_hP_A phase transition is clearly seen in dielectric studies. For all homologues a monodispersive relaxation process is observed in the Col_h phase (Fig. 4), with strength considerably increasing near the phase transition to the Col_hP_A phase. Most probably the relaxation mode originates in fluctuations deforming the nonpolar flat disks into polar cones; it is hereafter called the *umbrella* mode. This assumption is justified as the instantaneous phase structure that would be imposed by such fluctuations is polar and corresponds to a lower-temperature phase structure. The temperature variation of the relaxation frequency of the umbrella mode depends on the nature of the Col_h-Col_hP_A phase transition. For the homologues $n=8$ and $n=12$, which exhibit a strongly first-order phase transition, the umbrella mode relaxation frequency f_r follows a Vogel-Fulcher (VF) dependence [11] $f_r \equiv f_{VF}=f_0 e^{-D/(T-T_g)}$, where f_0 and D are constants and T_g is the glass transition temperature. The VF model is a generalization of the Arrhenius model, and is used for systems in which complete freezing of molecular motions occurs at $T_g>0$ K. For both $n=8$ and $n=12$ homologues, T_g obtained by fitting the VF equation to experimental data is several degrees below T_c. For the homologue $n=14$ the relaxation frequency of the umbrella mode shows a small departure from VF behavior in the low-temperature range of the Col_h phase; its decrease is faster

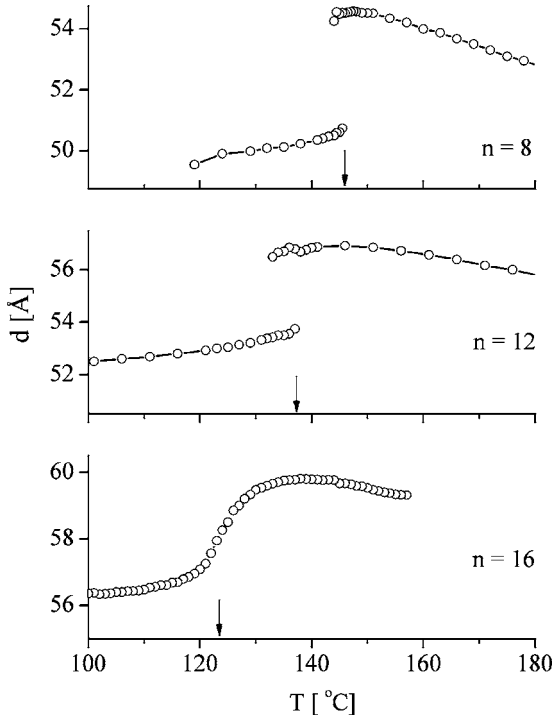

FIG. 2. Temperature dependence of (10) Bragg signal (measured on cooling) reflecting changes of the columns diameter. Discontinuous change is observed at the Col_h-Col_hP_A phase transition for $n=8,12$, while for the homologue $n=16$ the variation is continuous. Arrows indicate the Col_h-Col_hP_A phase transition temperature obtained from DSC measurements.

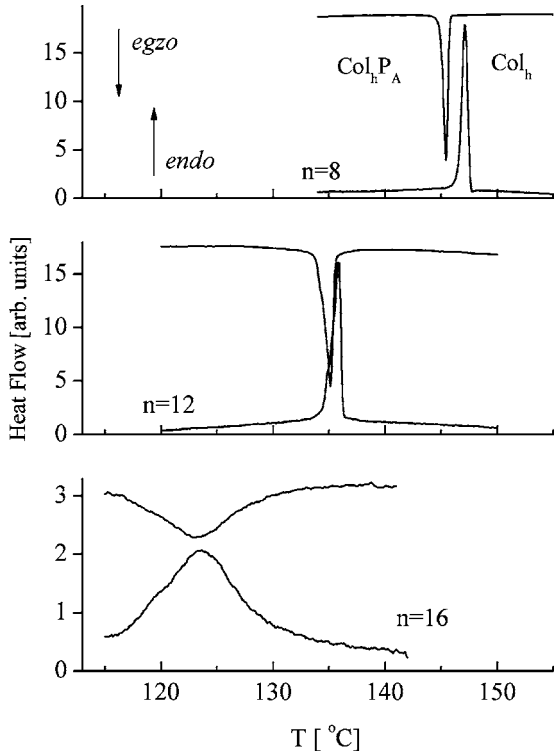

FIG. 3. DSC heat flow signals for homologues $n=8$, 12, and 16. The signals develop c_p wings and the hysteresis for heating and cooling scans diminishes as the terminal chains get longer.

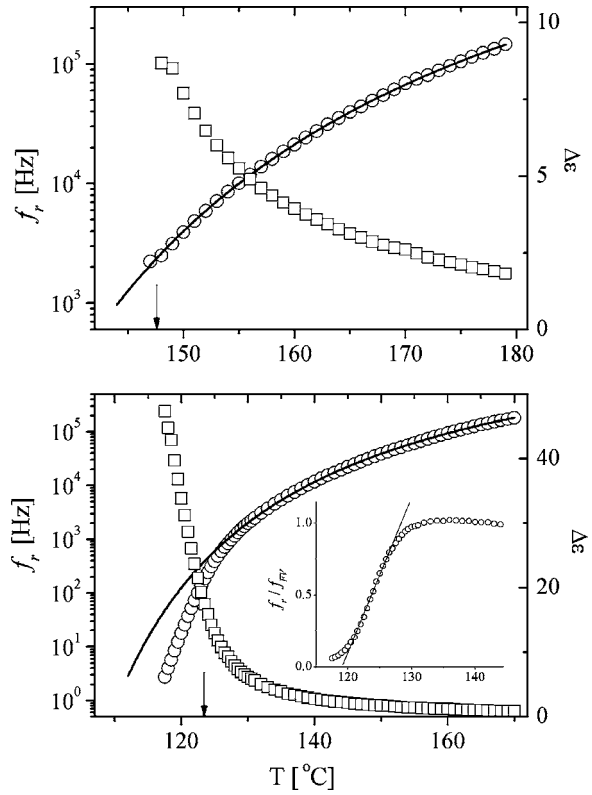

FIG. 4. Relaxation frequency (circles) and dielectric strength (squares) of umbrella mode in the Col_h phase vs temperature for homologues $n=8$ (upper graph) and $n=16$ (lower graph). The lines represent fits to the VF dependence. Arrows indicate the Col_h-Col_hP_A phase transition temperature obtained from DSC measurements. For $n=16$ in the vicinity of T_c crossover to the Curie-Weiss dependence takes place, as shown in the inset.

than predicted by VF behavior. For the homologue $n=16$, on lowering the temperature, the approach of the polar phase is manifested by rapid damping of the relaxation frequency and strong deviation from VF dependence. Near the phase transition f_r can be best described by a superposition of VF and Curie-Weiss dependence, $f_r=A(T-T_s)f_{VF}$ (see inset of Fig. 4), which characterizes systems in which the energy barrier for dipole reorientation under an electric field depends on temperature [11]. Such a coexistence of the critical slowing down and glassy freezing has often been considered for solid relaxors [12]. For materials $n=8-14$ in the Col_hP_A phase no low-frequency relaxation process can be detected, the umbrella mode is quenched exactly at the temperature at which the heat flow peak is observed in a differential scanning calorimetry (DSC) scan, and the diameter of columns discontinuously changes. Contrary to shorter homologues, in the material $n=16$ the relaxation process is not suppressed at the Col_h-Col_hP_A phase transition, it can be seen over several degrees below T_c. The temperature dependence of the dielectric response measured at different frequencies (Fig. 5) exhibits characteristic shifts of the maximum position and value of the dielectric susceptibility, which further confirms the existence of some slow, polar-active fluctuations in the lower-temperature phase.

The disk deformation into cones can be detected also by optical methods (Fig. 6). All observed phases are optically

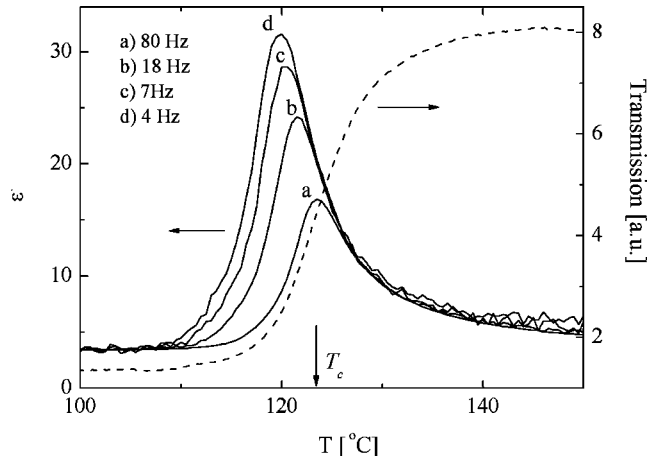

FIG. 5. Dielectric constant measured at different frequencies and simultaneously measured light transmission through a confocal domain in 3-μm-thick cell for homologue $n=16$. The high dielectric response is still visible below the T_c temperature.

uniaxial with optical axis along the column axis. In the Col_hP_A phase the optical birefringence decreases relative to the Col_h phase, as disk deformation increases the refractive index component along the column and decreases the component transverse to the column axis. Simple calculations show that the birefringence changes with cone angle β as

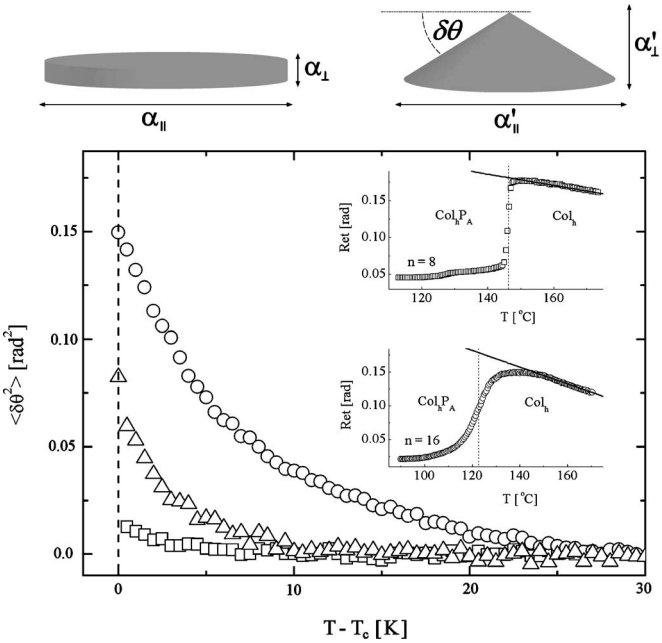

FIG. 6. Schematic drawing of column building blocks: Disks and cones. The change from flat disk to cone results in change of polarizability, $\alpha'_\parallel-\alpha'_\perp=(\alpha_\parallel-\alpha_\perp)[3\cos^2\delta\theta-2]$ and thus reduces the birefringence. Below: Mean square fluctuations of tilt angle vs temperature in the Col_h phase on approaching transition to the Col_hP_A phase, deduced from the birefringence measurements for homologues $n=8$ (squares), $n=12$ (triangles), and $n=16$ (circles). In the inset optical retardation vs temperature measured in 3.2 μm cell for the light propagating along a direction inclined by 30° from the column axis. Solid lines show noncritical part of retardation.

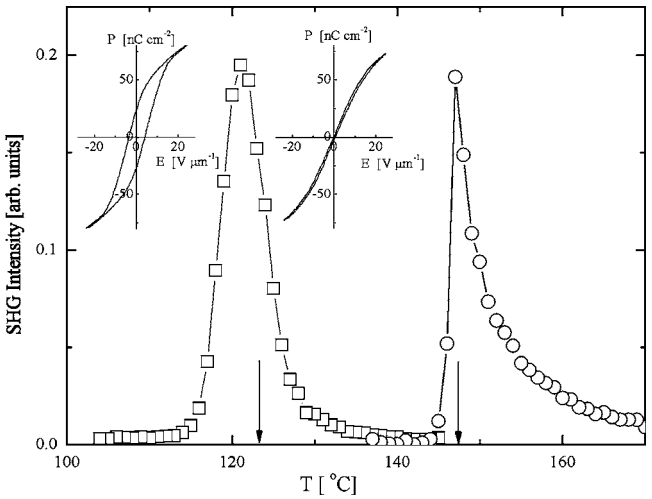

FIG. 7. Intensity of SHG signal vs temperature for homologue $n=8$ (circles) and $n=16$ (squares). The SHG signal increases in Col_h phase due to softening of the umbrella mode. Note the different signal decrease rates in $n=8$ and $n=16$ compounds. In the insets polarization hysteresis loop measured at 20 Hz in the $\mathrm{Col}_h P_A$ (at $T-T_c=-2$ K) and Col_h (at $T-T_c=4$ K) phases of $n=16$ compound showing different origins of electric-field-induced SHG signal in $\mathrm{Col}_h P_A$ phase (spontaneous electric polarization) and in Col_h phase (induced electric polarization). Single hysteresis loop in $\mathrm{Col}_h P_A$ phase is observed because of too slow relaxation to antiferroelectric ground state.

$3\cos^2[(\pi-\beta)/2]-2$. In all materials the $\mathrm{Col}_h P_A$ phase is nearly optically isotropic, which suggests a cone angle close to 110°. Along with results of x-ray studies, the change of birefringence at the Col_h-$\mathrm{Col}_h P_A$ phase transition is stepwise for compounds $n=8-14$, and the step decreases on elongation of the terminal groups. For the $n=16$ homologue a continuous change of birefringence through the phase transition is observed. The birefringence measurements are also used to monitor the umbrella fluctuations deforming the disks in the Col_h phase. Straightforward calculations (analogous to that performed for the smectic-*A* (Sm*A*) phase [13,14]) show that the birefringence is influenced by umbrella fluctuations as $\Delta n(T)=\Delta n_0(T)[1-3\langle(\delta\theta)^2\rangle]$, where $\pi-2\delta\theta$ is the instantaneous cone angle β (Fig. 1) and $\Delta n_0(T)$ is the noncritical part of the birefringence. In the Col_h phase, with decreasing temperature, the background part $\Delta n_0(T)$ increases as the orientational order in the column increases. Along with increasing umbrella fluctuations near the phase transition, the birefringence deviates downward from the extrapolation of data obtained far above the transition temperature (inset in Fig. 6). It can be clearly seen (Fig. 6) that $\langle(\delta\theta^2)\rangle$ increases with increasing homologue number; the deviation is pronounced for homologue $n=16$, whereas only a small deviation emerges for the $n=8$ compound before making the phase transition to $\mathrm{Col}_h P_A$. Although the exact analysis of fluctuations is difficult, as their magnitude depends on the chosen background $\Delta n_0(T)$, for the $n=16$ material the average amplitude of pretransitional fluctuations in the Col_h phase, $\sqrt{\langle(\delta\theta)^2\rangle}$, as high as 20° can be estimated. There are also visible pretransition changes of birefringence in the $\mathrm{Col}_h P_A$ phase near T_c. In this phase, however, it is not possible to separate the part of the birefringence changes due to the mean field change of cone angle and due to cone angle fluctuations.

Finally, the second-harmonic generation (SHG) method has been used to monitor the polar properties of the phases. It should be emphasized that all phases are SHG silent in the ground state. The result is consistent with paraelectric properties of the Col_h phase and the structure with compensated polarization of the $\mathrm{Col}_h P_A$ phase. The SHG signal becomes visible in the Col_h phase upon applying an electric field, which deforms the disks and induces finite polarization. The SHG intensity follows the square of the applied field, as predicted for paraelectric materials [15]. With decreasing temperature in the Col_h phase the induced nonlinear polarization becomes larger and attains maximal SHG intensity near the Col_h-$\mathrm{Col}_h P_A$ phase transition temperature (Fig. 7) as at this temperature susceptibility of the disks to the deformation is the highest. On further cooling in the $\mathrm{Col}_h P_A$ phase the signal diminishes due to insufficient voltage to assure full switching into the ferroelectric state. The difference between $n=8$ and $n=16$ compounds is clearly seen in Fig. 7; the maximum of the SHG signal appears at the phase transition for $n=8$ and disappears abruptly below the transition temperature, whereas for $n=16$ it appears below the phase transition temperature and diminishes gradually on cooling. The broad temperature range in the $\mathrm{Col}_h P_A$ phase of the $n=16$ homologue, which is SHG active under an applied electric field, may originate from the existence of polar clusters.

CONCLUSIONS

Summarizing, the experimental results show that the Col_h-$\mathrm{Col}_h P_A$ phase transition is associated with the change of the column building blocks from flat disks into cones, which allows for axial polarization of the columns in the $\mathrm{Col}_h P_A$ phase. In the $\mathrm{Col}_h P_A$ phase columns are arranged into a hexagonal lattice, with spontaneous electric polarization along the columns. The lack of SHG signal and low dielectric response together with polarization switching in an electric field unambiguously point to antiferroelectric structure of the phase. However, the simple antiferroelectric arrangement of columns should be excluded as it is incompatible with a hexagonal lattice of columns [16]. The model of the $\mathrm{Col}_h P_A$ phase described previously [9] involves breaking of the columns and forming blocks with reversed polarization direction. To satisfy close packing requirements, the blocks are shifted by half the lattice period in the plane normal to the columns axis. The other model that could also be considered assumes harmonic modulations of the cone angle β and thus polarization and density along the column axis. In this model antiferroelectric hexagonal lattice frustration is avoided by shifting the phase of the modulation between columns. The exact three-dimensional structure of the $\mathrm{Col}_h P_A$ phase is still to be elucidated.

The presented results of x-ray, dielectric, and optical studies confirm that development of polar order depends on the column interactions. Apparently, with broadening of the columns, alkyl shells formed by partially melted terminal chains, the steric interactions between columns weaken and

the columns become more susceptible to deformation. As a result the softening of the polar lattice motions in the Col_h phase is observed together with growing correlation length for dipole-dipole interactions within the column; finally rising fluctuations drive the Col_h-Col_hP_A phase transition to the second order for the $n=16$ homologue. For the $n=16$ material evolution from the paraelectric to polar phase is characterized by a diffused, rather than abrupt, structural phase transition. The presence of a strong, polar low-frequency mode and the lack of permanent polarization in the zero-field state (proved by absence of the SHG signal) in the Col_hP_A phase may suggest that, contrary to shorter homologues, the phase has an irregular antiferroelectric structure made of ferroelectric clusters with random distribution of polarization. In disordered ferroelectric regions of the Col_hP_A phase the dielectric relaxation occurs due to polarization reversal; also domain boundary motions contribute to the dielectric response. It should be stressed that although the physical properties of the Col_hP_A phase of the $n=16$ material seems to be reminiscent of solid relaxors, their origins are much different. Most solid relaxor phases are believed to be caused by compositional fluctuations [17] or defects [18].

EXPERIMENT

The detailed synthetic procedure for the studied materials will be described elsewhere. X-ray experiments were performed with a modified DRON diffractometer (Cu $K\alpha$ line) in reflection mode from one surface-free sample. The temperature stability was controlled with accuracy 0.1 K. Calorimetric studies were conducted with a Perkin-Elmer DSC-7 apparatus, with scanning rates ± 5 K min^{-1}. Dielectric measurements were done with Solartron Impedance Analyzer SI1260, samples were sandwiched in indium tin oxide–coated glass cells, 2–10 μm thick, and put in a Mettler FP82HT hot stage for temperature control. The same samples were used for light transmission and birefringence measurements, which were performed with a setup based on a He-Ne laser, photoelastic modulator PEM90, lockin amplifier EG&G 7265, and photodiode FLCE PIN20. SHG intensity was observed by the oblique incidence (45°) of a *p*-polarized fundamental wave from a neodymium-doped yttrium aluminum garnet laser (Surelite I; SLI-10 1064 nm, 10 Hz, 2 mJ/pulse) onto the 5 μm cells. *p*-polarized SHG was detected from the transmission direction at the maximum voltage of the triangular wave (10 Hz, 30 V_{pp} μm^{-1}) applied along the substrate normal.

ACKNOWLEDGMENT

The work was supported by KBN Grant No. 4T09A 00425 and Grants-in-Aid for Scientific Research (S) (16105003) by the Ministry of Education, Culture, Sports, Science and Technology, Japan.

[1] R. Meyer, L. Liebert, L. Strzelecki, and P. J. Keller, J. Phys. (France) Lett. **36**, L69 (1975).
[2] A. D. L. Chandani, E. Gorecka, Y. Ouchi, H. Takezoe, and A. Fukuda, Jpn. J. Appl. Phys., Part 2 **28**, L1265 (1989).
[3] H. Bock and W. Helfrich, Liq. Cryst. **12**, 697 (1992).
[4] G. Scherowsky and X. H. Chen, Liq. Cryst. **24**, 157 (1998).
[5] T. Niori, T. Sekine, J. Watanabe, T. Furukawa, and H. Takezoe, J. Mater. Chem. **6**, 1231 (1996).
[6] C. Tschierske and G. Dantlgraber, Pramana **61**, 455 (2003).
[7] K. Kishikawa, S. Nakahara, Y. Nishikawa, S. Kohmoto, and M. A. Yamamoto, J. Am. Chem. Soc. **127**, 2565 (2005).
[8] Y. Okada, S. Matsumoto, Y. Takanishi, K. Ishikawa, S. Nakahara, K. Kishikawa, and H. Takezoe, Phys. Rev. E **72**, 020701(R) (2005).
[9] E. Gorecka, D. Pociecha, J. Mieczkowski, J. Matraszek, D. Guillon, and B. Donnio, J. Am. Chem. Soc. **126**, 15946 (2004).
[10] L. E. Cross, Ferroelectrics **76**, 241 (1987).
[11] M. E. Line and M. Glass, *Principle and Applications of Ferroelectric and Related Materials* (Oxford University Press, Oxford, 2001).
[12] B. E. Vugmeister and H. Rabitz, Phys. Rev. B **61**, 14448 (2000).
[13] K. C. Lim and J. T. Ho, Phys. Rev. Lett. **40**, 1576 (1978).
[14] M. Skarabot, K. Kocevar, R. Blinc, G. Heppke, and I. Musevic, Phys. Rev. E **59**, R1323 (1999).
[15] R. W. Terhune, P. D. Maker, and C. M. Savage, Phys. Rev. Lett. **8**, 404 (1962).
[16] M. Harris, Nature (London) **399**, 311 (1999).
[17] H. Z. Jin, J. Zhu, S. Miao, X. W. Zhang, and Z. Y. Cheng, J. Appl. Phys. **89**, 5048 (2001).
[18] Y. Yoneda, N. Matsumoto, H. Terauchi, and N. Yasuda, J. Phys.: Condens. Matter **15**, 467 (2003).